Efficacy of Bubble Screens on Turbidity Control in Dredging

May 2021

Matthew Dowling (md1279@wildcats.unh.edu)
Sean Gillam (stg1008@wildcats.unh.edu)
Derek Goulet (djg1034@wildcats.unh.edu)
Magdalyn Kosalek (mjk1043@wildcats.unh.edu)
Michael Monahan (mm1634@wildcats.unh.edu)
Jason Robidoux (jbr1009@wildcats.unh.edu)

Project Advisor: Professor Tracy Mandel

Table of Contents

1. Introduction

1.1. Abstract

This project aims to test the efficacy of bubble screens in containing a density current with the goal of understanding if they are a viable substitute for physical silt curtains. Silt curtains are currently used to control turbidity levels during dredging and pose technical and environmental problems. Experimentation involved a tank that was designed and constructed with a lock mechanism that was released to create a density current. A bubble screen was created through a pneumatic system that allowed air to flow out of small holes in PVC tubing. A density current was formed by allowing the higher density current to flow toward fresh water with release of the lock. Quantitative data was extracted from flow visualization methods during the experiment to determine how effective the bubble screen was at containing a density current. Qualitative analysis was conducted on how well the bubble screen could prevent mixing between the two fluids.

1.2. Background

Dredging is the transport of sediments from one location to another underwater. Dredging may be carried out to maintain the depths of boating channels, remove contaminated sediments from areas where it negatively affects the environment or help coastal communities combat erosion and storm surges by increasing beach sizes. The dredging process greatly intensifies turbidity in the water, or the amount of suspended sediment in the water that causes it to become opaque. The increased turbidity caused by dredging can cause a myriad of environmental impacts. These impacts include, but are not limited to, clouding of water, smothering of aquatic flora and fauna, especially coral reefs, excessive nutrient transport, and disabling aquatic life from swimming through the area. Current practices to control turbidity levels during dredging include the use of silt curtains. Silt curtains are physical barriers that extend from the water surface to the seafloor to contain fine sediments within the boundaries of the dredging site [1]. While silt curtains have been effective in controlling turbidity, there are also many issues that arise with their use. Firstly, there can be gaps between each section and between curtains and the seafloor, allowing sediment to escape through [1]. Further, silt curtains are subject to damage throughout operations and recovery and often need repair, increasing the price of operation costs [1]. Lastly, when dredging is occurring in zones where there is other vessel traffic, there must be paid workers 24 hours a day to open and close the curtain as needed to allow the traffic through.

This poses an additional cost of thousands of dollars [2]. Though silt curtains have been useful, there are certainly complications that come with them.

An alternative approach to containing sediment within the bounds of a dredging site is the use of bubble screens. A bubble screen is known as a "pneumatic barrier," meaning that it actively uses pressurized air to maintain separation of two regions. Conversely, a silt curtain is a passive barrier, meaning it is simply a physical barrier that stays in place [3]. The main purpose of bubble screens is to manage sediment through discouraging sedimentation and transport of sediments. They have been used in some applications, including freshwater and marine re-diversion, oil pollution control, noise and shockwave attenuation, and wastewater treatment (refer to sources [1], [3], and [7] for examples). Although there is still more research to be done on the effectiveness of these bubble screens in field applications, there are some findings available from various research projects.

Mendzil carried out studies on the impact of micro bubble screens on sediment dispersal [3]. Mendzil created a linear air diffusion system to create microbubbles to be used in the bubble screen, as seen in Figure 1. She found that the weight of the system was enough for it to sit at the bottom of the water column without needing any additional weight to hold it down. Mendzil further concludes that when used in a line across a passage of water, bubble screens will create flow patterns that allow the sediment to rise with the bubbles. When bubble screens are placed in clusters throughout the cross-section of a water passage or basin, they will increase bottom flow to help disperse sediments that may rest on the bottom or on a given structure [3].

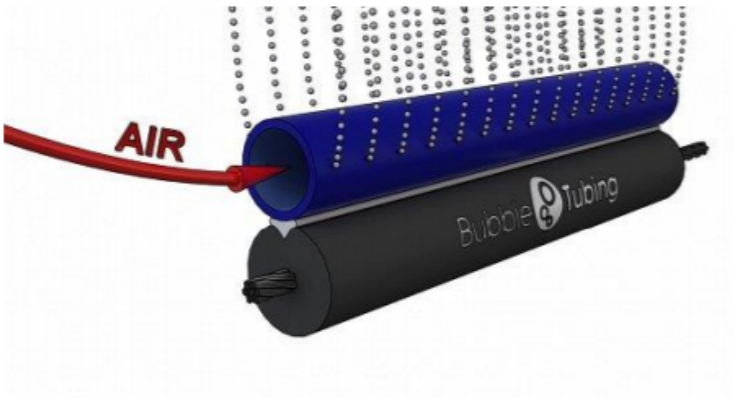

Figure 1: Bubble Tubing® schematic via VITA Water Technologies^{LTD} [3].

Tekeli and Maxwell have physically modeled bubble screens and found how they display certain desired behaviors [4]. The bubbles, while moving vertically upward throughout a water column, will exhibit forces on water particles, pushing them toward the surface. At the surface, a horizontal current is formed that moves away from this upward stream, as depicted in Figure 2. When producing a physical model of a bubble screen, it is important to scale the source strength properly to ensure the induced flow, velocities, and sizes of the bubbles are also properly scaled. The main source of scaling used is the Froude number scaling, as discussed in section 2.1 (Equation 2). Using different fluid types in the model than the prototype will help to achieve

similitude between them.

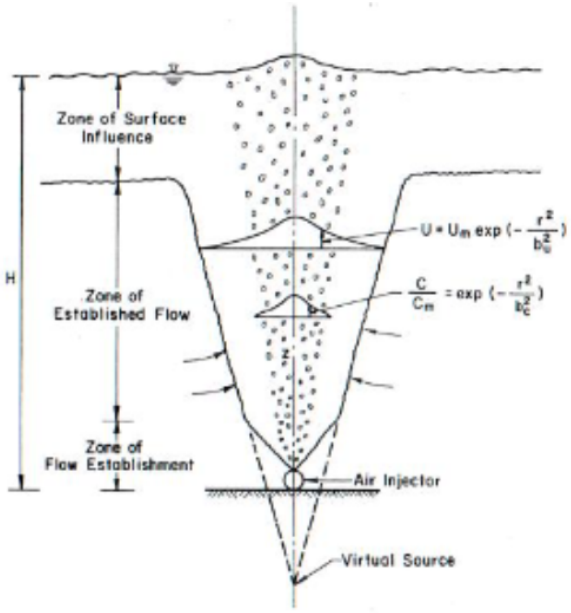

Figure 2: Schematic flow field for bubble plume [4].

1.3. Objectives

This project aims to test the efficacy of bubble screens in containing a density current with the goal of understanding if they are a viable substitute for silt curtains. A tank was designed and constructed with a lock mechanism acting as a release mechanism for a density current during experimentation. A bubble screen was placed along the cross-section of the tank below the lock, and a density current was created upon the release of the lock to simulate currents caused by the dredging of sediment. Quantitative data was extracted from flow visualization methods during the experiment to determine how effective the bubble screen is at containing the more dense fluid to its original side. Any significant observations on water mixing were noted and discussed. Experimental methods are expounded on in the *Methods* section.

1.4. Budget

The total budget for the project was set at $2200. Table 1, 2, and 3 outline all expenditures.

Table 1: Expenditures for tank construction and bubble screen tubing.

Tank				1			

Item	Location	Part #	Cost	Quantity	Shipping	Details	Total Cost per Item
Cast Acrylic	McMaster Carr	8560K273	$598.01	1	$100	8' x 4' x 0.5" Clear	$698.01
Weld-on Acrylic Applicator	Amazon	B0096TWKCW	$19.32	3	0	4 oz and needle applicator	$57.96
Silicon Sealant	Amazon	B0001FFLUI	$13	1	0	GE Sealants & Adhesives GE5040 Advanced Silicone 2 Kitchen & Bath Sealant, 10.1oz, Clear	$13
Epoxy	McMaster Carr		$42	1	8.83		$51
Aluminum Angle Stock	McMaster Carr	8982K4	$8	1		3'x1"x1" 1/8"wall	$8.32
Aluminum Angle Stock	McMaster Carr	8982K4	$5.78	4		2'x1"x1" 1/8 wall	$23.12
Aluminum Box Tubing	McMaster Carr	6546K53	$28.00	2			$56.00
Plastic Sheet	McMaster Carr	8574k54	$35.65	1		24”x24”x3/16”	$35.65
High Strength Acrylic Adhesive	McMaster Carr	7467A86	$14.03	3		Metal/Plastic/ composites	$42.09

Table 2: Expenditures for bubble screen construction

Curtain							
Item	Location	Part #	Cost	Quantity	Shipping	Details	Cost per Item
Pneumatic Cylinder	Mc-Master Carr	6498K449	$130	1	30	24" stroke	$160
Lexan Sheet	Mc-Master Carr		$50	1			$50
Air Hose	Mc-Master Carr	5280N11	$45	1		6mm ID, 25 ft	$45
Check Valves	Mc-Master Carr	7768k22	$13	4		1/4" NPT, 0.7	$52
Ball Valve	Mc-Master Carr	4085t21	$16.29	1		1/2"-1/4" NPT	$16.29
Pressure Gauge	Mc-Maste	4089k61	$20.77	1		Pipe Size 1/4"	$20.77

	r Carr						
Pipe Nipples	Mc-Master Carr	1867n12	$5.20	2		2" Long, 1/4" NPT	$10.40
Hose barb Adapter	Mc-Master Carr	5372K841	$6.47	1		6mm to 4mm, 10 pkt	$6.47
NITRA manual valve	Automation Direct	EVP-AS-PL	$19.00	1		2 port 4mm inlets	$19.00
Pneumatic Tubing	Automation Direct	PU532BLK100	$12.50	1		4mm OD tubing	$12.50
Hose Barb	Automation Direct	BAHB-316-18N	$9.50	5		3/16" hose to 1/8 Male NPT	$47.50
3/4 PVC CAP	Home Depot	611942038534	$0.68	11	0	3/4" cap slip	$7.48
3/4"X1/2" GAL COUPLING	Home Depot	19442148720	$3.24	2	0	3/4"X1/2"	$6.48
1/4" BARB X 1/4" FIP ADAPTER BRASS	Home Depot	887480002096	$3.27	1	0	1/4" Barb x 1/4" fip	$3.27
1/2"X1/4" BLK BUSHING	Home Depot	19442146702	$2.12	2	0	1/2"x1/4" bushing	$4.24
1/4" black tee	Home Depot	19442147648	$3.26	1	0	1/4" black tee	$3.26
1/4"X2" BLK NIPPLE	Home Depot	19442154288	$1.64	1	0	1/4"X2" BLK NIPPLE	$1.64
1/4" FP BALL VALVE	Home Depot	820633959717	$8.72	1	0	FPT 600PSI	$8.72
1"X1/2" BLK COUPLING	Home Depot	19442147280	$3.67	2	0	1"X1/2" BLK COUPLING	$7.34

Table 3: Expenditures for experimental materials and testing supplies.

Experimental Materials							
Item	Location	Part #	Cost	Quantity	Shipping	Details	Cost per Item
Food Dye	Amazon	B07VJM115H	$12.98	1		12 bottles 10ml	$12.98
Petroleum Jelly	Amazon	B07SKXXPMZ	$3.00	1		White 7.5 oz	$3.00
250ml Plastic Graduated Cylinder	Amazon	B075JNC466	$8.00	1		250ml Plastic Graduated Cylinder	$8.00

Hydrometer	Amazon	B076VTR4ZX	$15.09	2		Specific Gravity Range 0.700 to 2.000-0.01	$30.18
Hydrometer heavier than water	Amazon	B00LVU04ZE	$30.25	1		1.000/1.600 Specific Gravity	$30.25
Instant Ocean	Amazon	B000255NKA	$12.59	4		50 Gallon bag	$50.36
Loctite putty	Amazon	B074R72PSH	$23.87	1		2 oz 12 pack	$23.87

Table 4: Total expenditures for Efficacy of Bubble Screens on Turbidity project.

Total Cost			
Initial Funds	Tank	Curtain	Experimental Materials
$2,200	$1,467.13	$482	$152
Total Cost	Remaining Funds		
$2,108	$92		

Out of the total allowable budget of $2,200, approximately $2,110 were used. This gave a remaining budget of about $90. The remaining budget can be used for more experimental data as well as replacement parts for the tank and pneumatic system. Great Lakes Dredge & Dock provided an NTU sensor that they previously owned. Though the sensor was not used, it may be helpful in the future as the project continues.

2. Theory

2.1. Froude Number Scaling

The Froude Number (Fr) is a nondimensional number that represents a balance between the inertial and gravitational forces in a fluid and can be used for similarity relationships [4]. Froude numbers in dredging applications can vary from subcritical flow to supercritical flow (where the Fr can be less than or greater than 1). A Froude number larger than one indicates a steeper sloping gravity current, where a Froude number of less than one indicates a shallow sloping gravity current [5], illustrated in Figure 3.

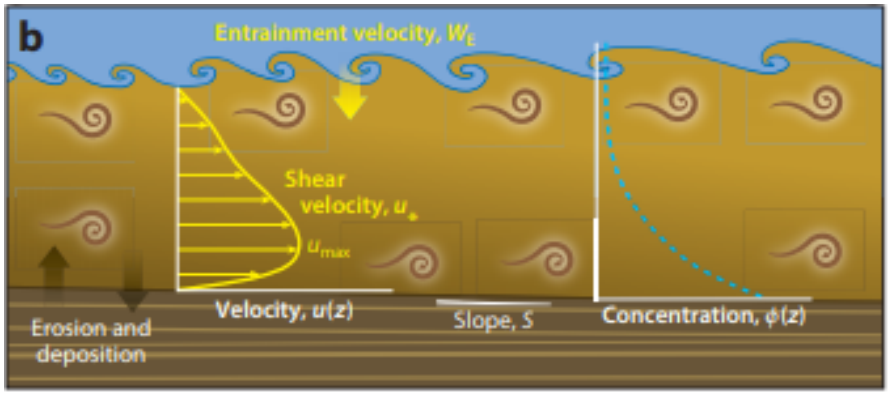

Figure 3: A graphic showing mean flow from a gravity current and how the slope is defined [5].

Using this relation, supercritical flow is synonymous to a steep sloping gravity current, and subcritical flow is synonymous to a shallow sloping gravity current. The experimental setup had no slope coming from the environment, so subcritical flow was expected.

Expecting a shallow slope with subcritical flow leads to a desired Froude number less than 1. Froude numbers greater than one would be non-physical for the experiment and represent some external circulation current within the test environment. Refer to section 4 for further discussion regarding Froude numbers greater than one and their implications given the experimental setup. The Fr number for scaling the density current is shown in Equation 1 [4].

$$\boldsymbol{Fr} = \frac{\bar{\boldsymbol{u}}}{\sqrt{\boldsymbol{g'h}}} \ \boldsymbol{(1)}$$

$$where:$$
$$Fr: Froude\ Number$$
$$\bar{u}: depth\ averaged\ velocity\ \left(\frac{m}{s}\right)$$
$$g' = g\left(\frac{\Delta\bar{\rho}}{\rho_o}\right)\ ;\ \left(\frac{\Delta\bar{\rho}}{\rho_o}\right) = relative\ density\ difference\ \left(\frac{m}{s^2}\right)$$
$$h: height\ of\ gravity\ current\ (m)$$

A gravity current is an imposed fluid motion as a result of a horizontal density gradient [4]. This drives a more dense fluid to sink below the less dense fluid. The relative density difference is between the turbid fluid and freshwater (where one side of the tank will have turbid fluid held by a lock between the other side with freshwater). The depth averaged velocity is to be calculated and the height of the gravity current is to be determined through flow visualization.

The bubble screen itself also has an associated Froude number, which is shown in Equation 2 [5]. The Froude number calculated for the bubble screen would be used to then scale the screen (through submerged depth and discharge rate) for field applications.

Scaling of Bubble Screen

$$Fr_q = \left(\frac{q_a^2}{g' H^3}\right)^{\frac{1}{3}} \quad (2)$$

$$where:$$
$$Fr_q: densimetric\ Froude\ number\ (2D\ plume)$$
$$q_a: discharge\ rate\ per\ unit\ length\ for\ air\ \left(\frac{m^2}{s}\right)$$
$$g' = \left(\frac{\Delta\overline{\gamma_a}}{\rho_w}\right);\ \left(\frac{\Delta\overline{\gamma_a}}{\rho_w}\right) = relative\ density\ difference\ \left(\frac{m}{s^2}\right)$$
$$H: depth\ of\ injector\ submergence\ (m)$$

The discharge rate per unit length was estimated [4] and the height of the depth of injector submergence was measured. The dynamics of a full bubble plume system are described by several nondimensional numbers, of which Froude is only one. Scaling the pressure non dimensional number for discharge rate per unit length was not feasible given a lack of necessary equipment. The results might be an overestimate by not appropriately scaling depending on actual discharge rate, where Tekeli mentioned possibilities of being off by factors of ~4 between prototype and models [4]. It is noted that getting an accurate discharge rate is difficult. The density difference is much greater than the environmental case (~1000 kg/m^3), Resulting in relative differences of ~9.78 m/s^2. The Froude number defined in equation (2) is used to show a densimetric relationship between a bubble plume source strength and surrounding freshwater (singular fluid). This Froude number would be used for scaling purposes of the bubble screen when implemented into the field..

The Froude number of the bubble screen can also be related to the mitigation of dense/turbid fluid (in this case salt), as found through a numerical study conducted by Oldeman et al. [6]. The authors compared field test data, experimental results, and numerical simulations of a salt transmission factor (the amount of salty water passing through the screen) as a function of an Froude number (shown below is Figure 21 from their findings) to classify salt intrusion of the bubble screen, shown in equation (3).

Classification of Bubble Screen

$$Fr_{air} = \frac{(q_a g)^{1/3}}{(g' H)^{1/2}} \quad (3)$$

$$where:$$
$$Fr_{air}: Froude\ number\ of\ screen$$
$$q_a: discharge\ rate\ per\ unit\ length\ for\ air\ \left(\frac{m^2}{s}\right)$$
$$g' = \left(\frac{g\Delta\rho}{\rho_s}\right)\ relative\ density\ difference\ \left(\frac{m}{s^2}\right)$$
$$H: depth\ of\ injector\ submergence\ (m)$$

The classification Froude number (3) can be thought of as a ratio of flow inertia induced from the air that flows into a system to the external fluid field. Note that the new relative density difference uses the difference between salt and freshwater, where saltwater is the reference density (ρ_s). This Froude number was used for classification of the bubble screen to predict the effectiveness against intrusion of salt through the screen.

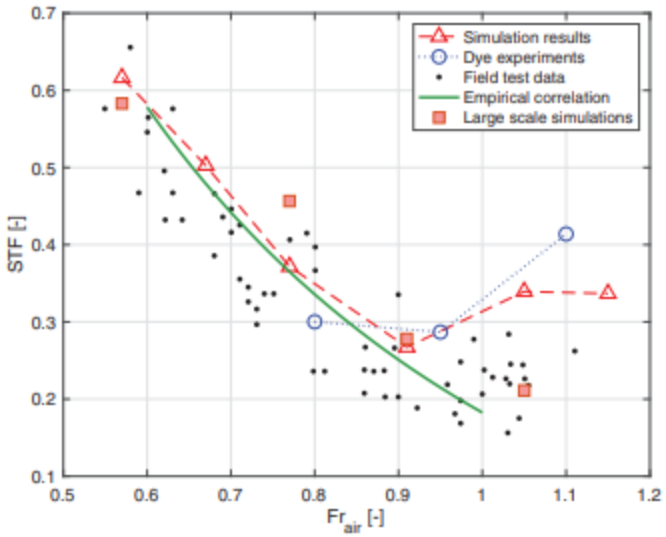

Figure 4: Salt transmission factor (STF) modeled as a function of Froude number of the bubble screen from [6]. Refer to references within their report for data collection.

The mitigation of turbid fluid as a function of Froude number for the bubble screen exhibits a concave up parabolic effect when classified as subcritical and supercritical when

looking at simulation results (red triangles on Figure 4). It was found through numerical simulation that there is an optimal Froude number of ~0.91 [6]. Increasing subcritical Froude numbers of the bubble screen (< 0.91) and supercritical Froude numbers (> 0.91) both show increased turbid fluid transmission through the screen. However, the cause behind the increase of transmission for each case is different. For subcritical classification Froude numbers, the screen is not producing a great enough concentration of bubbles to contain the gravity current and turbid fluid. For supercritical Froude numbers, turbulent mixing at the surface occurs, promoting transmission of turbid fluid past the screen location [6].

The Froude number of the environment (1) is crucial for experimental purposes to adhere to the subcritical flow classification, where the Froude number of the bubble screen is to serve as a basis for future work when implemented in field scenarios (2), and the classification Froude number (3) was used to compare visual results to predicted salt intrusion. The Froude number of the screen would be held constant upon implementation into the field (given the field environment is also subcritical flow).

The subcritical flow environmental Froude number is meant to serve as a baseline for future studies. Iterations can be performed to vary expected Froude numbers (like the introduction of slopes to the environment).

2.2. Data Analysis: Techniques

The different parameters that were varied include depth averaged velocity and current height (through density difference between the two fluids), discharge rate per unit length of bubble screen (through pressure regulator valve), and the orientation and number of holes in bubble screen orifice design (up to 7 iterations).

Orientation and the number of holes in the bubble screen had an iterative design, as discussed in section 3.1.4. The optimal design was chosen through flow visualization experiments.

A consistent Froude number was the primary goal through all experimentation, which was calculated to be on the order of magnitude of 1 [5]. A Froude number of 1 was used to estimate parameters such as mean flow rate of turbid current and discharge rate of the bubble screen prior to each trial. An actual Froude number was calculated post-trial using recorded depth averaged velocity of the gravity current (3) and discharge rate per unit length of the bubble screen (in line flow meter).

If a trial had the correct order of magnitude Froude number of less than one, it was concluded that the trial could confidently be used for determining the effect of varying the mentioned parameters (height, mean flow velocity, discharge rate of bubble screen). For trials that met the criterion, a visual comparison was conducted using snapshots of side by side footage of time series recordings, such as in Figure 5.

Conclusions were made on how different heights and depth-averaged velocities of the density current and varying discharge rate per unit length of the bubble screen tubing affect the efficacy of a bubble screen for dredging applications. Figures 5 and 6 show expectations of

depth-averaged velocity changes corresponding to different current heights and Froude scaling values using equation 1 for density differences of 20 and 15 kg/m^3.

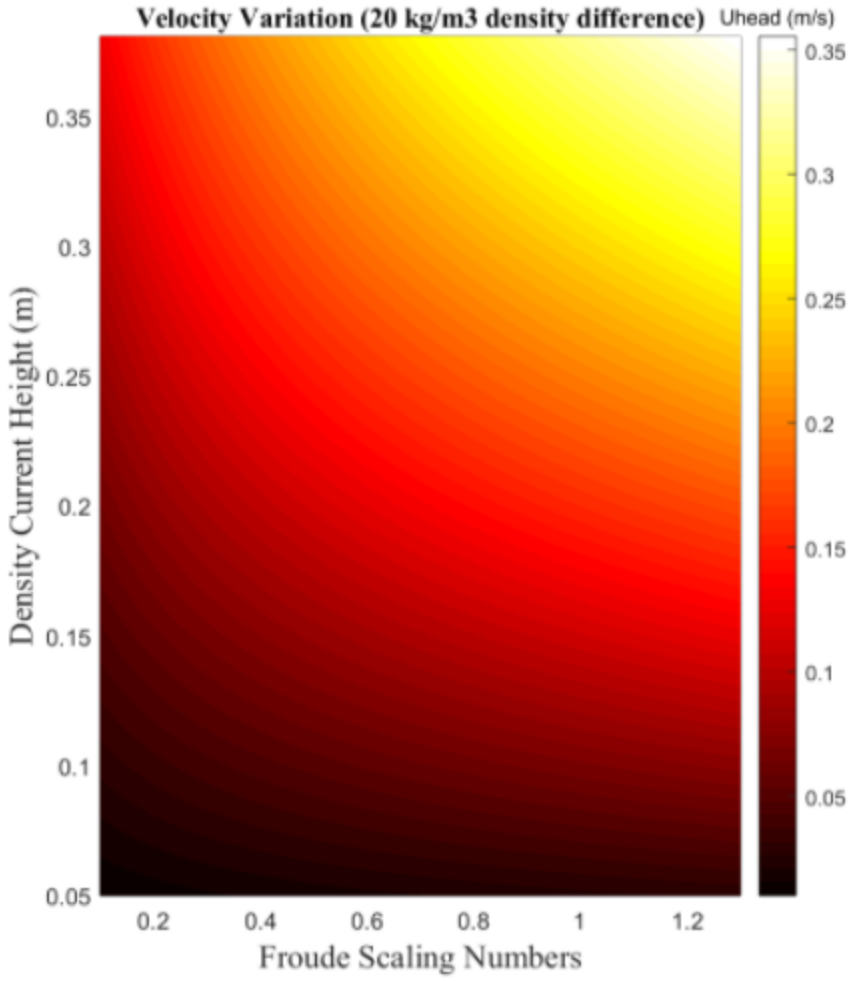

Figure 5: Pseudocolor plot showing variation of depth averaged velocity values for different combinations of current height and froude scaling value. This uses a density difference of 20 kg/m^3 between the salt and fresh water in equation 1.

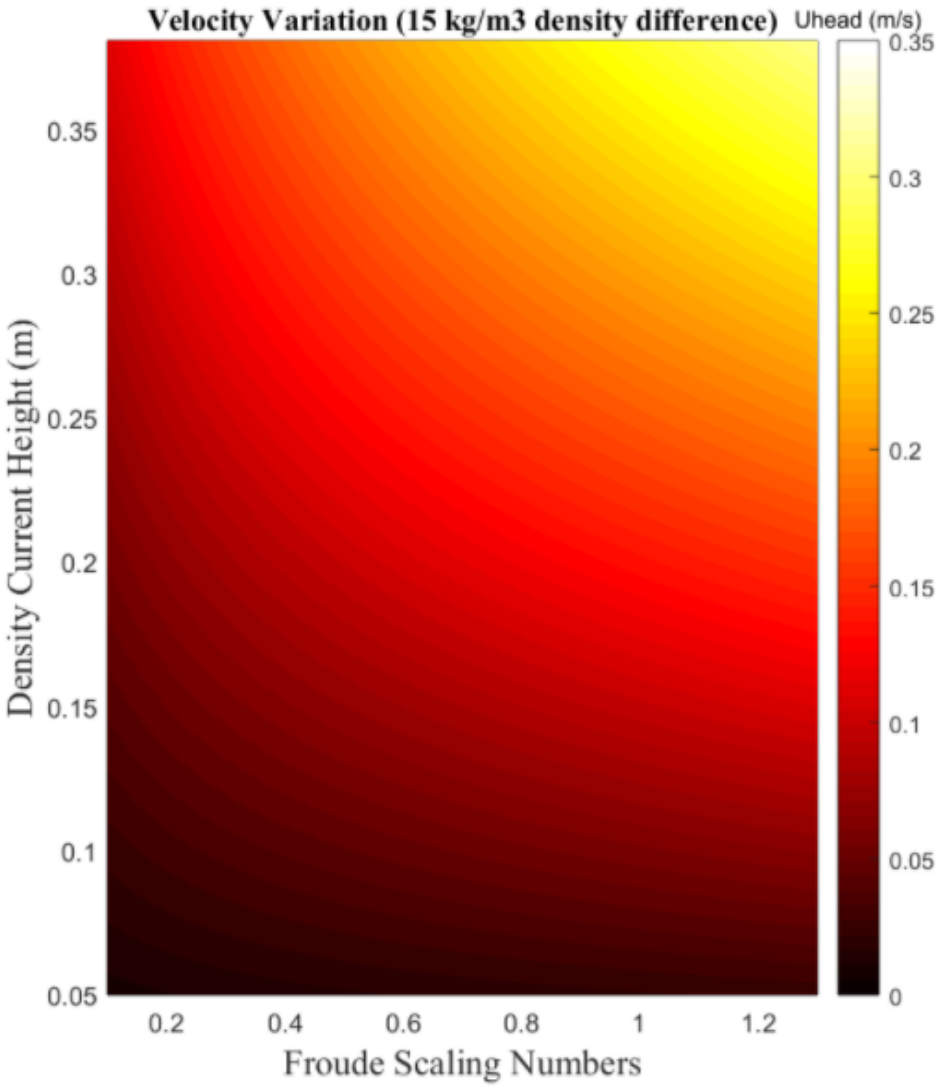

Figure 6: Pseudocolor plot showing variation of depth averaged velocity values for different combinations of current height and froude scaling value. This uses a density difference of 15 kg/m^3 between the salt and fresh water in equation 1.

3. Methods

3.1. Material Design and Construction

3.1.1. Tank

The tank was constructed using 0.5 inch thick cast acrylic. The tank was constructed such that the inside dimensions were 16in x 24in x 48in. The walls of the tank were secured together and to a base sheet of acrylic using acrylic adhesive. For an increase in strength and support, four triangular pieces of acrylic were cut and secured to the walls of the tank using the acrylic

adhesive. Two supports were applied to either side. To aid in making the tank watertight, GE Sealants clear silicone caulk was applied to all inside edges of the tank. For reinforcement, ¼" aluminum angle stock was attached to the outside corners. The aluminum was attached using acrylic-aluminum epoxy.

The sides of the tank were broken into a salty, dense water (left) and ambient fresh water (right). The heavier-density was created by using Instant Ocean until a density of approximately 1015-1025 kg/m^3 was reached.

The bubble screen configurations were secured into the freshwater side of the tank and also attached to the in house air supply run at either 10 or 20 psi (depending on trial). Plumbers putty was used to secure the bubble screen into the water, while easily allowing for swapping of respective bubble screens across experiments.

3.1.2. Lock Mechanism

To create a density current in the tank, an adjustable lock barrier was installed. The lock barrier was set up in the middle of the tank with an aluminum support frame holding up a pneumatic piston as shown below in Figure 7. This piston was then connected to an acrylic sheet that slides down in the middle of the tank and is designed to split the tank lengthwise into two separate watertight chambers. To prevent premature mixing of the different density waters, a gasket was placed around the edge of the lock to ensure it was water tight. Water with different densities based on salt content was poured on each side of the barrier to a height of 43 cm. Quick release of the lock using the pneumatic piston causes the higher density fluid to flow toward the lower density fluid, resulting in a density current. This current was observed by dyeing the high density fluid. The full design for the tank and lock mechanism is found in Figure 7.

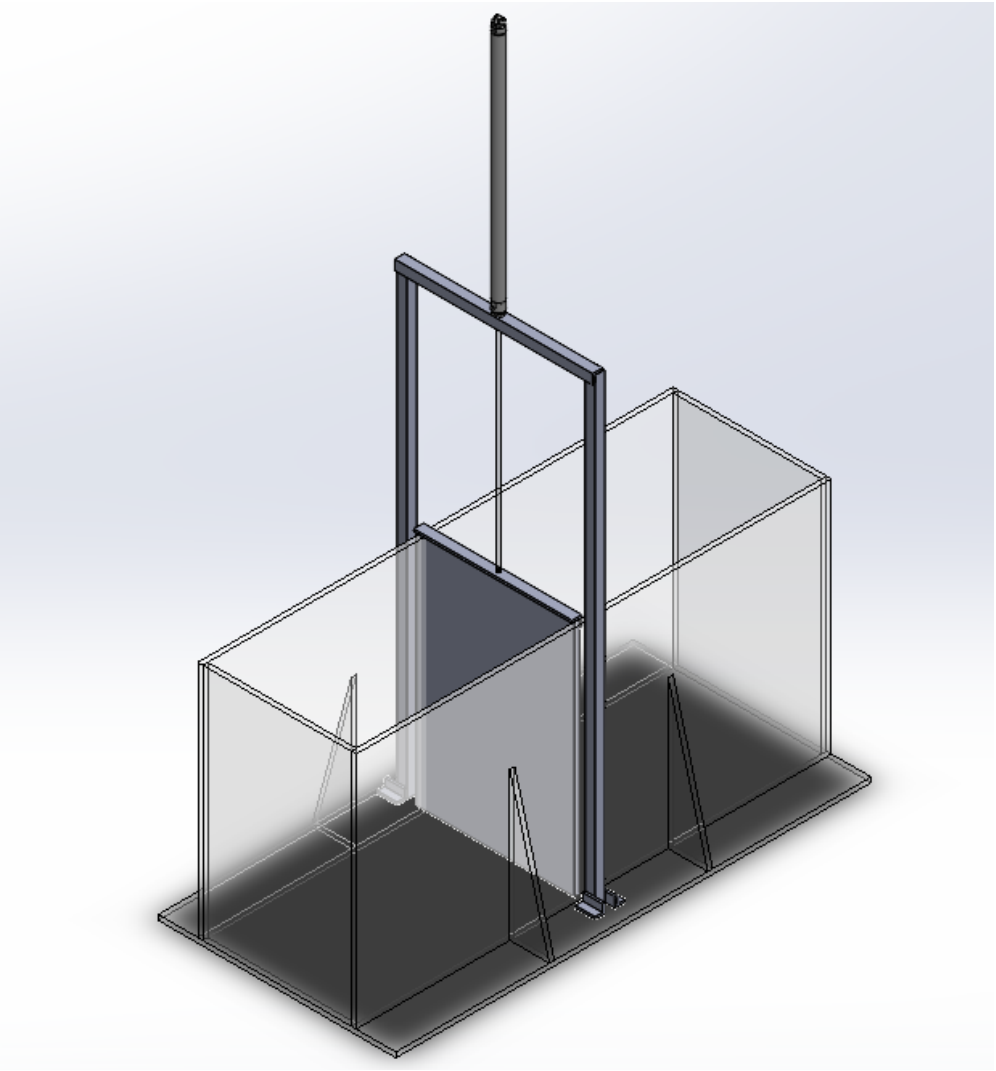

Figure 7: SolidWorks model of tank and lock mechanism design.

3.1.3. Pneumatic System

The majority of the pneumatic system can be seen below in figure 8. Starting from the bottom of the figure is the connection to the in house air supply with the pressure at the source regulator set to 25 psi. The supply is then directly connected to an aluminum buffer tank which ensures that regardless of pull from the system, the air flow to the bubble screen will be constant. Moving up from this buffer tank is a T joint which leads to a ball valve to the left and a second regulator on the right. The ball valve releases air into the pneumatic cylinder which then lifts the lock. The regulator on the other branch of the system is used to control the pressure of the bubble curtain. It was significant that the piston received 25 psi as this is the pressure necessary to lift the lock in a repeatable manner.

Guides were installed on either side of the lock to ensure strictly vertical motion and repeatability across all trials conducted. Vaseline was used on the walls of the tank to reduce the friction as the gate is lifted vertically.

Figure 8: The pneumatic system for the experimental setup. The bottom right is a connection to the building air supply.

3.1.4. Bubble Screen Tubing

The bubble screen tubing was made of PVC piping with a ¾ inch inside diameter. Several different orifice design configurations were tested, and all were 16 inches long (Figure 9). For each different design, the tubing was placed along the bottom of the tank in the less dense fluid, directly under the lock barrier. The integrated air system in the Jere A. Chase building was used to provide air flow through the bubble tube over a range of 10 to 20 psi, where the connection is shown at the bottom of Figure 8 (most trials were restricted to 10 psi). The in house air lock was released, and the two release valves at the top of Figure 8 could be opened to allow air flow to the lock (left, blue handle) or bubble screen (right, black dial). Each of the tested orifice design configurations are depicted and described in the figures below.

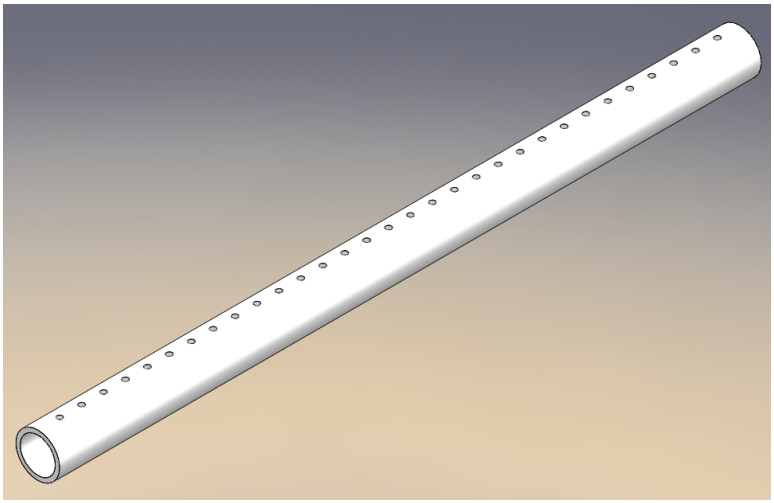

Figure 9: A SolidWorks model of a basic hole configuration. There are ⅛” holes spaced ¼” on center between adjacent holes. The holes total to a count of 31.

For the first configuration mentioned in Figure 9, there was also an iteration done with ⅛” on center spacing. This had a total count of 61 holes throughout.

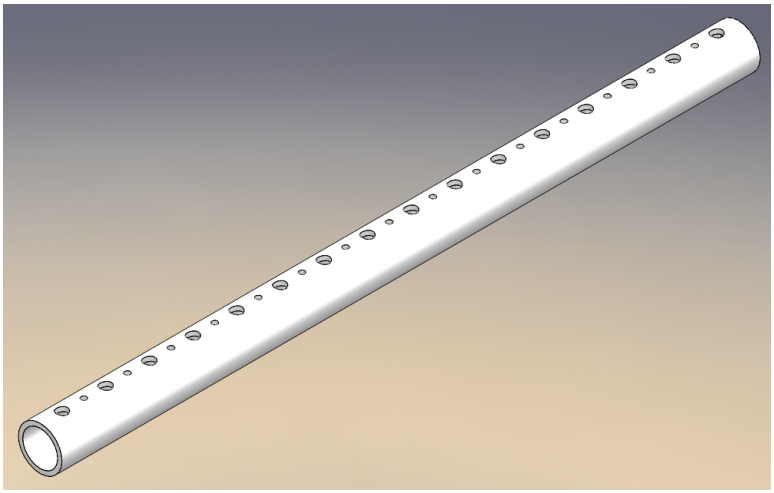

Figure 10: A SolidWorks model of an alternating hole configuration. There are alternating ¼” and ⅛” holes spaced ½” on center (¼” on center between adjacent holes). The holes total to a count of 31.

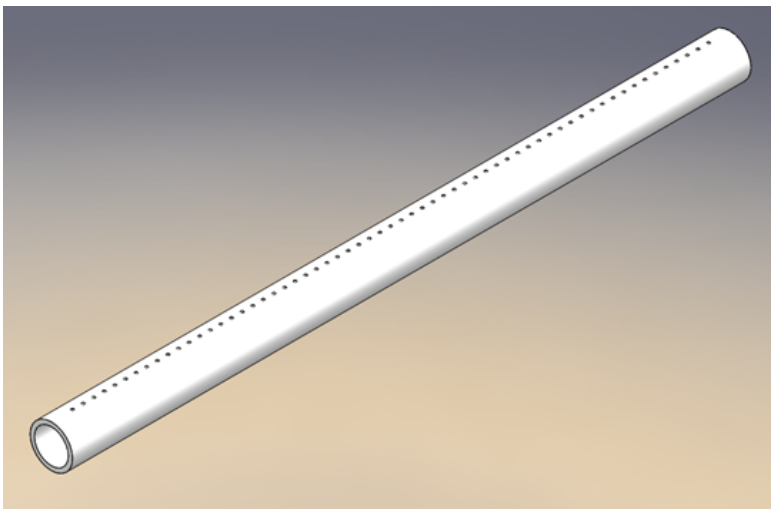

Figure 11: A SolidWorks model of the finalized bubble screen with 1/16” holes spaced ¼” on center. The holes total to a count of 61.

The bubble screen configurations were compared visually, with the configuration shown in Figure 11 being the optimal choice based on the ability to produce a uniform bubble curtain with minimal water surface turbulence while efficiently containing the imposed gravity current. Other configurations required greater supply pressures to operate, causing significant turbulent mixing on the surface of the water. Alternatives also had too great of a spacing between bubbles to produce a uniform screen. The configuration in Figure 11 would be used for the trials conducted.

Each tube received two ¾” end caps that were secured with PVC cement. To apply air to the bubble screen, a ½” hole was drilled into the tube and tapped with a ¼” NPT thread. A one way valve was secured into the hole and made watertight. This allowed for a one way valve, while reducing water flowing into the pneumatic system. Air was supplied from the pneumatic system rated at 10 or 20 psi (depending on trial).

Refer to Section 5.1 for discussion on the process of determining the final bubble screen iteration to be used and Section 5.2 for discussion on the Froude number estimation of the bubble screen.

3.2. Creating a Density Current

For dredging applications, there are a multitude of differing environments where the work may be conducted. A dredging site may have a shallow or steep slope, and no two are exactly alike. For the experiment, the same type of gravity current will be recreated each trial, where the Fr number of the gravity current will be held constant to observe the efficacy of a bubble screen for a “mid-range” case of slope steepness.

The depth averaged velocity, V_{avg}, will be estimated by the mean velocity of the gravity current through flow visualization, shown in equation (4).

$$V_{avg} = \frac{\Delta x}{\Delta t} \quad (4)$$

In equation (4), Δx is the horizontal distance traveled by the leading edge of the gravity current before reaching the bubble screen, and Δt is the time it takes for the leading edge to travel this distance.

With the lock mechanism in place, two separate chambers are created in the tank. Water with different densities based on salt content was poured on each side of the barrier to a depth of 20 inches. Once the lock mechanism was released, the higher density fluid could flow toward the lower density fluid, creating a density current. The lock mechanism was controlled with a pneumatic system to ensure repeatability and precision. The current was observed by dyeing the high density fluid different colors such that the mixing of the two sides could be qualitatively assessed. Two monochrome (black and white) cameras were used to record the current and allow for post-processing of the images.

3.3. Acquiring Quantitative Data

3.3.1. Environment - Velocity, Flow Height, and Density Differences

The profile imaging acquired from experiments was inspected frame-by-frame to calculate the average velocity of the density currents. A line of best fit was measured from the tracking of the leading edge of the density current. Through dividing the distance this leading edge traveled in the tank by the corresponding time, an average velocity estimate was calculated (Equation 1). The following graphic (Figure 12) shows a snapshot in time of a trial where quantitative information can be gathered through visualization.

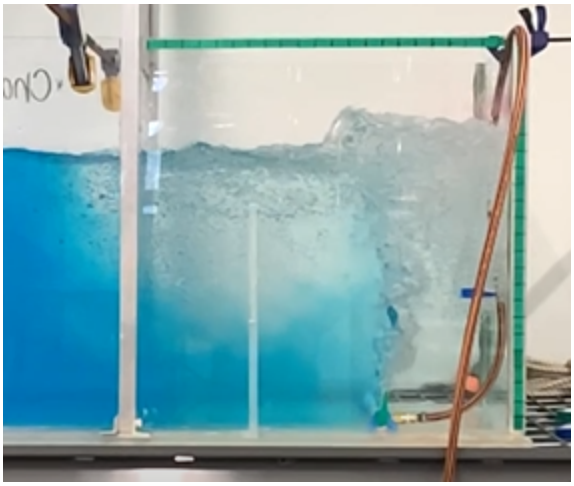

Figure 12: Image showing density current reaching bubble screen. Scaling references with an inch spacing are seen on the sides of the tank.

The height of the gravity current was determined through flow visualization as well. The green tape shown in Figure 12 has scaling references with spacing of an inch. The scaling

references were used to measure the average flow height of the density current and the distance traveled over a given time of the density current. Note that the flow height is taken as the distance from the bottom of the tank to the middle of the gravity current.

A hydrometer was used to calculate densities of the different fluids needed for calculations. The hydrometer was placed in the salty-solution side of the tank to measure the density of the water. The fresh water density was measured with the hydrometer to be 1000 kg/m^3, and the salt water densities used for screen scaling were 1015 and 1020 kg/m^3, respectively. The density difference was taken and compared to the reference density of freshwater to find the relative density difference (after multiplying the ratio by gravity).

3.3.2. Screen - Depth, Discharge rate, and Density Difference

Values were found to determine the Froude scaling of the bubble screen using equation 2. The depth of water in the tank was 0.43 m. Oldeman et al. [6] varied discharge rate over a range of 10-100 L/min (1e-04-1e-03 m^3/s) for an almost equal depth case (0.4 m used for their experimentation). An in line flow meter was out of the bounds of the budget, so an order of magnitude approximation was used. The following method was used to predict the discharge rate from the screen per unit length of screen (16 inches, 0.4 m).

Supercritical classification Froude numbers (indicative of >0.91 with turbulent surface mixing) were seen during experimentation. For approximately equal densities and depths, this corresponded to flow rates on the order of 100 L/min for Olderman et al. [6]. On this basis, 100 L/min was used as an estimated order of magnitude for the discharge rate of the bubble screen. Discharge rate per unit length was then calculated to be 0.005 m^2/s as a result.

The density difference for the scaling Froude number was calculated using the same methodology discussed in section 3.3.1, except it was now the difference between freshwater and air. The fresh water density was measured with the hydrometer to be 1000 kg/m^3, and the density of air in the room was estimated to be 1.2 kg/m^3 based on environmental conditions at time of experimentation. The density difference for the classification Froude number was calculated using the same method as section 3.3.1, but the reference density was now the salt water.

3.3.3. Camera Configuration

High-speed monocolor cameras (refer to Appendix section 8.2) were used for the recording of experimentation. Images of the density current were taken at 15 frames per second (fps). The amount of frames observed over a certain distance of flow could then be divided by this fps to determine the time. The images were analyzed to estimate a depth averaged velocity and flow height. These values were used for determination of the experimental Fr number.

3.4. Preliminary Experimentation

To ready the tank for experimentation and ensure all parts were in working order, the experiment was run without the bubble screen in place. The lock mechanism was clamped in

place in the center of the tank to create the two equal control volumes. One control volume was filled with freshwater and the other was filled with salt water of a recorded density (refer to section 3.3.1). The saltwater chamber was dyed with food coloring to allow for flow visualization as the two sides interacted. The depth of each side was recorded before the release of the lock to compare with the depth of the turbid fluid after the release, and their differences were noted. The two monochrome cameras were prepared and mounted in place to record the experiment. The actuators were run and the lock was lifted. The result of the density current mixing with freshwater was visually seen and observations were made. The initial experiment was performed to ensure that the denser fluid would create a density current when mixing with freshwater.

3.5. Final Experimentation

Working parts were verified in preliminary experimentation and the bubble screen tubing was installed in the freshwater side of the lock using plumbers putty and secured to the pressured air source. The bubble screen was turned on prior to release of the lock, where it would reach a steady state of operation. Steady state was defined by a visual confirmation of a uniform bubble curtain produced by the orifice, where there was no visual variance in the screen for ~6-8 consecutive seconds. Reaching steady state took on the order of 10 seconds for each experiment. The lock was released, and the same visualization techniques highlighted in section 3.3.1 were utilized.

The different bubble screen orifice configurations (refer to section 3.1.4) were tested and compared visually against a constant gravity current. Once an optimal configuration was identified, other parameters could be varied and observed. Multiple trials were conducted varying the depth and relative density difference of the two fluids by adding more or less water and salt, respectively. The discharge rate of the bubble screen was created through a pressure supply from the pneumatic system over a range of 10-20 psi.

Observations such as gravity current penetration of the bubble screen, turbulent surface mixing, and any other significant visual effects were noted. Refer to section 5.2 for more discussion on possible discrepancies between experiments.

4. Results

4.1. Density Current Scaling

Table 4: Tests to determine sufficient gravity current

Bubble Screen	Current Height	Froude Scaling	High Density	Low Density	Depth Averaged	Depth Averaged

Present	(m)	Value	(kg/m^3)	(kg/m^3)	Velocity (expected) (m/s)	Velocity (observed) (m/s)
No	0.2	0.3	1015	1000	0.06	0.05
Yes	0.127	0.48	1020	1000	0.05	0.076
Yes	0.2	1.27	1020	1000	0.17	0.25
No	0.15	0.5	1020	1000	0.07	0.1

Ideal depth averaged velocities were calculated for the experimental results using figures 4 and 5. These values were then compared to the observed depth averaged velocities for the four experiments conducted, with and without a bubble screen implemented. The depth averaged velocities were greater with the bubble screen implemented. This observation is discussed further in section 5.2.

4.2. Bubble Screen Scaling & Classification

Bubble screen scaling values were calculated using a density difference of ~999 kg/m^3, respectively, in equation (2). The Froude scaling number of the bubble screen was calculated to be 0.03. The depth of the bubble screen was 0.43 m for the estimated air flow of 0.005 m^2/s. The scaling bubble screen value would be used to implement the screen into field scenarios.

The classification bubble screen Froude number was also calculated, where the density difference between the two ambient fluids was now used [6] from equation (3). The density of the fresh water was 1000 kg/m^3 and the saltwater ranged from 1015-1020 kg/m^3. The same estimated flow rate of 0.05 m^2/s was used with a height of 0.43 m to calculate a classification Froude number of ~1.27 (using 1020 kg/m^3 as this was the mode). The classification Froude number is indicative of supercritical flow, matching the visualization experiments.

5. Discussion

5.1. Finalization of Bubble Screen

Bubble screen orifice designs mentioned in section 3.1.4 were compared. It was found that larger holes led to increased turbulence at the surface, which was undesired for the experimental situation as it led to increased mixing. Larger holes also required greater air pressure to create a uniform bubble curtain.

Alternating holes produced no significant differences when compared to holes of the same size along the length of the tubing. As alternating would complicate fabrication of the bubble screens for an indifferent result, it was determined not to use them for further experimentation.

Further iterations of the screen were created, where smaller holes were used with less spacing in between. Smaller hole spacing and size correlated with an increased efficacy of preventing the gravity current penetration of the screen. The smaller holes also produced less turbulent mixing at the water surface, helping to prevent any denser fluid from mixing into the freshwater reservoir.

A lower limit of 1/16” hole size was reached (any smaller and the material would not have clean cut holes), with a spacing of ¼” on center. This was considered the optimal configuration, where it is noted that a smaller on center spacing of ⅛” could be tested but believed to not have a significant difference. Smaller spacing was confirmed to not make as significant a difference as hole size through trials across varying iterations of the bubble screen orifices.

A discharge rate of 0.005 m^2/s (refer to section 3.3.2 for reasoning) was used to estimate an order of magnitude classification Froude number for the bubble screen of ~1.27. The theoretical optimal Froude number of 0.91 is less than the classification Froude number calculated for the bubble screens [6]. This is indicative of purely supercritical flow, where the mixing occurs primarily at the surface due to turbulence.

5.2. Froude Variance - Turbulence and Circulation

The classification Froude number represented supercritical flow for the air out of the screen. Through flow visualization, it was determined that the main mode of salt water transmission was through the turbulent mixing at the surface, which is reflective of Froude numbers greater than 0.91 [6]. The bubble screen effectively stopped the penetration of the gravity current through the screen itself.

There is an insignificant difference between the estimated number and the visualization conclusions made for the classification Froude number of the bubble screen as both visualizations and predicted value of 1.27 represented supercritical flow. There is confidence in both the height of the bubble screen and relative density difference as those quantities were directly measured. There is confidence in using 0.005 m^2/s as an estimated discharge rate per unit length of the screen as Olgeman et al. [6] had almost exactly the same experimental setup for turbid fluids, depth of water, and supercritical flow visualization. The difference to be noted is the unit length, where 0.5 m was used as a length scale to normalize discharge rate in Olgeman et al.’s experimentation. The visualization experiments conducted match the theoretical Froude number as there is significant turbulent mixing occurring, giving confidence in the methodology of determining an order of magnitude discharge rate of the screen. Error could stem from the estimation however, where it would be recommended in future work to invest in a device that measures this discharge rate directly.

Although the screen can be experimentally classified as supercritical bubble screen flow, this is above the desired Froude number of 0.91, which leads to increased transmission of salt to the freshwater reservoir in the tank. To reduce the turbulent surface mixing and bring the containment up the discharge rate could be lowered through regulating the pressure to below the supplied 10 psi, more turbid fluid could be used, or the depth of the bubble screen could be increased. Either option would decrease the effective Froude number of the bubble screen, getting closer to the optimal of 0.91 and improving containment of turbid fluid.

When analyzing the turbulence throughout the water column, it became clear that at the surface where turbulence is creating, mixing occurs. Another method of reducing the turbulence was explored, where bubble screens were created with smaller holes, such as ⅛" and ¼" OC. With this alteration a great deal of turbulence was still created at the surface. To reduce the turbulence even more at the surface, a regulator was added in series with the bubble screen. The regulator allowed for a variation in the rate of discharge and the quantity of bubbles produced. With this addition, the flow was able to be reduced to minimize turbulence at the surface while keeping a constant flow through the water column.

There is confidence in the Froude number order of magnitude for the bubble screen as the visualization experiments matched predicted characteristics of the experiment. However, the Froude number for the environment experienced great variance. The depth averaged velocity of the density current increased with the bubble screen present. This was due to a circulation current being formed adjacent to the bubble screen due to a pressure drop across the tank. This circulation current could be seen by dropping dye in the tank next to the lock while it was closed and the bubble screen was running. With the tank filled with only freshwater, the dye was observed to continuously move in a circular motion next to the bubble screen, proving this screen-induced current was present (Figure 13). This dye eventually mixed with the other side of the bubble curtain due to turbulence at the top of the water. In a field application of a bubble screen, this circulation current may be minimal compared to the size of the density current. However, it was shown to have a significant effect on the depth averaged velocity of the experiments conducted in a tank, which is a closed basin.

Figure 13: Image taken from video of circulation current formed due to the pressure drop induced by the bubble screen.

6. Conclusion

6.1. Experimental Conclusion

Determining the efficacy for bubble screens in controlling turbidity currents can be limited when only performed in a laboratory environment. A gravity current is simulated from one side of the control environment, where the other is stagnant water with no induced current. This is not reflective of all real world dredging applications. Environments can drastically differ, where water can be flowing in the same direction as the induced gravity current, against it, or occasionally be stagnant [7]. Only the stagnant case was studied here.

From the stagnant case, the bubble screen has potential as a means of stopping a gravity current induced by sediment from escaping a control area. Through experimentation, the bubble screen stopped the gravity current, where the only mixing into the fresh water reservoir was caused through turbulent mixing at the water surface. Varying the pressure, making the bubble screen “less aggressive,” reduces this turbulent mixing that occurs at the surface.

The design of the bubble screen went through various iterations of hole size, supply pressure, and hole spacing until an optimal configuration was determined through flow visualization experiments. The optimal configuration used was 1/16” holes spaced ¼” on center

with a desired supply pressure of 10 psi. This reduced surface turbulence relative to other screen iterations, while providing a uniform screen of bubbles throughout the whole width of the tank.

The bubble screen could be implemented in specific environments such as the stagnant ambient fluid mentioned, but performance could fall off drastically upon changing environments. This is significant as many dredging applications occur in environments where the water is ever changing with tides, winds, etc. This could pose many risks as the bubble screen could amplify mixing given certain conditions.

6.2. Future Work

The purpose of this project was to start a partnership with Great Lakes Dredge and Dock while observing the efficacy of bubble screens on turbidity control. There are a lot of potential avenues to continue this work and build upon the relationship with GLDD. Future work could include exploring different relative density differences by using actual sediment from project sites and observing the overall effect (like any changes of the Froude number order of magnitude).

For the first year of the project, the main goal was to build a repeatable experiment that held a constant Froude number from trial to trial. In the coming years, experiments can be conducted to observe the effect of varying parameters such as water height, depth averaged velocity, discharge rate of the bubble screen, etc.. while trying to maintain a consistent Froude number. An alternative could be taken where parameters are varied with the intention of getting different Froude numbers, where the goal would be to best predict the bubble screen response in shallow ($Fr < 1$) or steep environments ($Fr > 1$) [5]. This information could better estimate the necessary bubble screen configuration for a given dredging environment.

One way to improve data analysis would be to create MATLAB code that can take a video file as input and extract the parameters to calculate & output a Froude number and characterize the experiment as a shallow, steep, or potential anomaly. This would decrease analysis time immensely and allow for continuous experimentation over a semester.

A significant problem with the current experimental setup is the induction of turbulence from the bubble screen, where the bubbles eventually induce mixing of both sides and create high frequency surface waves (see Figure 12).

Possible solutions could include varying the angle of attack of the bubble screen orifice to limit turbulent mixing. It is noted that the surface was where any escape of sediment occurred for the experimental setup discussed. It has been concluded that the bubble screen effectively stops gravity currents from penetrating the vertical column of air itself, but there was surface turbulent mixing that occurs.

7. References

[1] JC Ogilvie, D. Middlemiss, MW Lee, N. Croussouard, and N. Feates, "Silt curtains - a review of their role in dredging projects," *HR Wallingford,* [Online], Available: https://eprints.hrwallingford.com/865/1/HRPP560_Silt_curtains_-_a_review_of_their_role_in_dredging_projects.pdf [Accessed March 10, 2021].

[2] R. Ramsdell. "RE: Rescheduling of Meeting." Personal Email (Nov. 19, 2020).

[3] A. Mendzil, "Micro bubble curtains: impact on Sediment Dispersal," *SEACAMS2 Project (SC2-R&D-SU03)*. Swansea University, pp. 19, 2018.

[4] S. Tekeli & W.H.C. Maxwell, "Physical Modeling of Bubble Screens," *Journal of the Waterway Port Coastal and Ocean Division,* Feb., pp. 48-64, 1980.

[5] M.G. Wells & R.M. Dorrell, "Turbulence Process Within Turbidity Currents," *Annual Review of Fluid Mechanics,* pp. 53:59-83, 2021.

[6] A.M. Oldeman, S. Kamath, M.V. Masterov, T.S.D., O'Mahoney, G.J.F van Heijst, J.A.M Kuipers, and K.A. Buist, "Numerical Study of Bubble screens for mitigating salt intrusion in sea locks," *International Journal of Multiphase Flow,* May 3, 2020.

[7] M. Nakai & M. Arita, "An Experimental Study on Prevention of Saline Wedge Intrusion by an air Curtain in Rivers," *Journal of Hydraulic Research*, 40:3, 333-339, Feb. 2010. [Online], Available: https://doi.org/10.1080/00221680209499947 [Accessed April 7, 2021].

[8] P. Kundu, I. Cohen, and D. Dowling, *Fluid Mechanics*. Waltham, MA: Academic Press, 2012.

[9] MAE. Class Lecture, Topic: "Gravity Currents." School of Engineering, University of California, San Diego, CA. [Online], Available: http://maeresearch.ucsd.edu/linden/MAE/ch5_04.pdf [Accessed April 5, 2021].

8. Appendix

8.1. Datasheets

Instant Ocean (https://m.media-amazon.com/images/I/81aluoTpf4L.pdf):

Instant Ocean Sea Salt

Instructions:

1. Mix Instant Ocean® with ordinary dechlorinated tap or purified water.
NOTE: To prepare small quantities, use 1/2 cup of Instant Ocean per each U.S. gallon of water. Mix as directed.

2. Stir vigorously to ensure a good mix. Although the Instant Ocean solution may be used immediately, we suggest aerating the water until it achieves oxygen/carbon dioxide equilibrium.

3. Measure specific gravity with an Instant Ocean® Hydrometer.

Recommended Specific Gravity Range: 1.020 - 1.024 at 77°F.
NOTE: 1.5 lbs of Instant Ocean is formulated to create 5 gallons of saltwater at a specific gravity of 1.022.

4. Adjust salt level accordingly. If specific gravity is too low, add more Instant Ocean. If too high, add more dechlorinated water.
5. Change 20% of aquarium water every two weeks to maintain optimum water quality.

USAGE NOTE: NEVER mix salt in an aquarium containing animals.

In New Aquariums:
Transfer animals to the aquarium AFTER salt is completely mixed and aerated and specific gravity has been adjusted.

CAUTION: INSTANT OCEAN IS NOT FOR HUMAN CONSUMPTION. KEEP OUT OF REACH OF CHILDREN.
Contact in dry form may cause skin or eye irritation.
In case of contact, completely flush skin or eye(s)
with cool water and seek medical attention.

Monochrome Cameras
(https://www.flir.com/products/blackfly-s-usb3/?model=BFS-U3-28S5M-C)

SPECS	BFS-U3-28S5M-C	BFS-U3-28S5C-C
Resolution	1936 x 1464	
Frame Rate*	130 FPS	
Megapixels	2.8 MP	
Chroma	Mono	Color
Sensor	Sony IMX421, CMOS, 2/3"	
Readout Method	Global shutter	
Pixel Size	4.5 µm	
Lens Mount	C-mount	
ADC	10- bit / 12-bit	
Minimum Frame Rate**	1 FPS	
Gain Range**	0 to 47 dB	
Exposure Range**	10 µs to 30 s	
Acquisition Modes	Continuous, Single Frame, Multi Frame	
Partial Image Modes	Pixel binning, decimation, ROI	
Image Processing	Gamma, lookup table, and sharpness	Color correction matrix, gamma, lookup table, saturation, and sharpness
Sequencer	Up to 8 sets using 6 features	
Image Buffer	240 MB	
User Sets	2 user configuration sets for custom camera settings	
Flash Memory	6 MB non-volatile memory	
Opto-isolated I/O	1 input, 1 output	
Non-isolated I/O	1 bi-directional, 1 input	
Auxiliary Output	3.3 V, 120 mA maximum	
Interface	USB 3.1 Gen 1	
Power Requirements	8 - 24 V via GPIO or 5 V via USB3 interface	
Power Consumption	4.2 W maximum	
Dimensions/Mass	29 mm x 29 mm x 39 mm / 53 g	
Machine Vision Standard	USB3 Vision v1.0	
Compliance	CE, FCC, KCC, RoHS, REACH. The ECCN for this product is: EAR099.	
Temperature	Operating: 0°C to 50°C Storage: -30°C to 60°C	
Humidity	Operating: 20% to 80% (no condensation) Storage: 30% to 95% (no condensation)	
Warranty	3 years	

*Frame rates are measured with Device Link Throughput Limit of 380 MBps and Acquisition Frame Rate disabled. Values are rounded down to whole numbers.

**Values are the same in binning and no binning modes.